Small-angle neutron scattering and molecular dynamics structural study of gelling DNA nanostars

J. Fernandez-Castanon, F. Bomboi, L. Rovigatti, M. Zanatta, A. Paciaroni, L. Comez, L. Porcar, C. J. Jafta, G. C. Fadda, T. Bellini, and F. Sciortino

Citation: The Journal of Chemical Physics **145**, 084910 (2016); doi: 10.1063/1.4961398
View online: http://dx.doi.org/10.1063/1.4961398
View Table of Contents: http://scitation.aip.org/content/aip/journal/jcp/145/8?ver=pdfcov
Published by the AIP Publishing

Small-angle neutron scattering and molecular dynamics structural study of gelling DNA nanostars

J. Fernandez-Castanon,[1] F. Bomboi,[1] L. Rovigatti,[2,3] M. Zanatta,[4,5] A. Paciaroni,[4] L. Comez,[4,6] L. Porcar,[7] C. J. Jafta,[8] G. C. Fadda,[9] T. Bellini,[10] and F. Sciortino[1,5,a)]
[1]*Sapienza–Università di Roma, P.le A. Moro 5, 00185 Roma, Italy*
[2]*Rudolf Peierls C.T.P., University of Oxford, 1 Keble Road, Oxford OX1 3NP, United Kingdom*
[3]*Faculty of Physics, University of Vienna, Boltzmanngasse 5, A-1090 Vienna, Austria*
[4]*Dipartimento di Fisica, Università di Perugia, Via Pascoli, 06123 Perugia, Italy*
[5]*CNR-ISC, UOS Sapienza–Università di Roma, I-00186 Roma, Italy*
[6]*IOM-CNR, UOS Perugia c/o Dipartimento di Fisica e Geologia, Università di Perugia, Via Pascoli, 06123 Perugia, Italy*
[7]*Institut Laue-Langevin, 71 Avenue des Martyrs, CS 20156, 38042 Grenoble Cedex 9, France*
[8]*Helmholtz-Zentrum Berlin, Hahn-Meitner-Platz 1, 14109 Berlin, Germany*
[9]*Laboratoire Léon Brillouin, LLB, CEA Saclay, 91191 Gif-sur-Yvette Cedex, France*
[10]*Department of Medical Biotechnology and Translational Medicine, Università di Milano, I-20133 Milano, Italy*

(Received 5 May 2016; accepted 5 August 2016; published online 31 August 2016)

DNA oligomers with properly designed sequences self-assemble into well defined constructs. Here, we exploit this methodology to produce bulk quantities of tetravalent DNA nanostars (each one composed of 196 nucleotides) and to explore the structural signatures of their aggregation process. We report small-angle neutron scattering experiments focused on the evaluation of both the form factor and the temperature evolution of the scattered intensity at a nanostar concentration where the system forms a tetravalent equilibrium gel. We also perform molecular dynamics simulations of one isolated tetramer to evaluate the form factor numerically, without resorting to any approximate shape. The numerical form factor is found to be in very good agreement with the experimental one. Simulations predict an essentially temperature-independent form factor, offering the possibility to extract the effective structure factor and its evolution during the equilibrium gelation. *Published by AIP Publishing.* [http://dx.doi.org/10.1063/1.4961398]

I. INTRODUCTION

The development of new *smart nanomaterials*,[1,2] i.e., materials able to adapt their nanoscale response to different external stimuli, is central in many scientific and technological fields, including medicine,[3–5] drug-delivery,[6–8] photonics,[9,10] and computing.[11,12] The desoxyribonucleic acid (DNA) is one of the most promising materials to encompass the aforementioned applications. Its base pairing specificity (A···T, G···C) allows for detailed control over the design of deliberated structures. The molecule responsible for storing our genetic information, something as natural as life itself, startlingly provides the perfect ingredient to create new functional materials[13,14] via a cascade of self-assembly processes, each one guided by the length of complementary sequences of distinct DNA strands.

One of the first DNA constructs which has been designed and realized in the lab[15] is the DNA nanostar (NS) with controlled valence f. Here, the word valence indicates the maximum number of bonds that a particle can form, and it is the analog of the word *functionality* in chemical reactions.[16] To build the structure, f properly designed DNA single strands are mixed together in equimolar concentration. The sequence design favours the pairing of each strand with two different partners, in such a way that a construct with a flexible, unpaired core and f double-helical arms is spontaneously formed (see Fig. 1). A self-complementary short sequence at the end of each arm provides the sticky site to bind distinct NSs. This methodology allows for the synthesis of supramolecular constructs in macroscopic quantities, opening the way for an experimental study of their bulk behavior. NS particles have been selected as optimal candidates for testing the role of the valence on the gas-liquid phase separation.[17,18] Consistent with theoretical studies[19,20] it has been shown that these particles undergo a phase-separation process between a phase of isolated NSs and a network phase, in which NSs bind to form a thermoreversible gel, the physical correspondent of f-functional chemical gels.[21]

Differently from the chemical case, the equilibrium phase behavior of this system can be explored. Beyond the coexisting density, on cooling, the system moves continuously from a high-temperature (T) state in which monomers only interact via their excluded volume (and eventually electrostatic) repulsion to a fully bonded low-T state (the equilibrium gel) via a progressive formation of larger and larger aggregates. The possibility to break and reform bonds makes it possible to release stresses and reach at low T a fully bonded state, e.g., a gel free of entanglement and defects.

a)Author to whom correspondence should be addressed. Electronic mail: francesco.sciortino@uniroma1.it

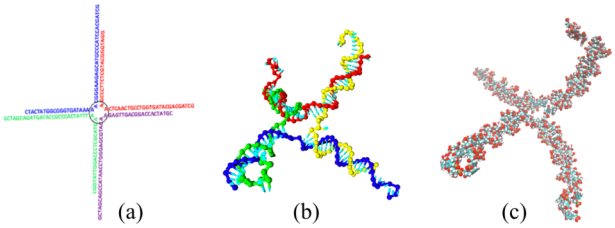

FIG. 1. Representation of a NS at different levels. (a) The four sequences of bases forming the NS. Each single strand has been represented with a different color. Note the six unpaired bases, acting as sticky ends; (b) the oxDNA representation of the self-assembled NS, in which each base is modelled as a rigid body; (c) the corresponding full atom representation.

Dynamic light scattering (DLS) experiments[18,22] of the DNA-gel formation have shown that the density fluctuations relax slower and slower on cooling, following an Arrhenius T dependence, increasing by more than five orders of magnitude in a small T interval, before exiting from the accessible experimental time window (10 s). Here, we present a series of Small-Angle Neutron Scattering (SANS) experiments carried out to quantify the structural signatures associated with the formation of the equilibrium gel at a selected concentration. As T is decreased, the system evolves from fluid to gel through a succession of equilibrium steps, without the interference of phase separation. We also present experiments at a much lower concentration, where the form factor of the NS can be measured. We complement the experimental study with a numerical investigation of the structure of a single NS, based on the coarse-grained oxDNA2[23] model. This provides an effective way to connect the observed signatures in the SANS diffraction pattern with geometrical parameters. The quality of the experimental data and the agreement with the numerical form factor allow us to extract an effective structure factor between the centers of the NSs under the hypothesis of decoupling between translational and orientational degrees of freedom.

II. MATERIALS AND METHODS

A. Materials and sample preparation

The four sequences programmed to self-assemble in tetravalent DNA-NSs are

Sequence 1. 5′-CTACTATGGCGGGTGATAAAAA
CGGGAAGAGCATGCCCATCCA**CGATCG**-3′
Sequence 2. 5′-GGATGGGCATGCTCTTCCCGAA
CTCAACTGCCTGGTGATACGA**CGATCG**-3′
Sequence 3. 5′-CGTATCACCAGGCAGTTGAGAA
CATGCGAGGGTCCAATACCGA**CGATCG**-3′
Sequence 4. 5′-CGGTATTGGACCCTCGCATGAA
TTTATCACCCGCCATAGTAGA**CGATCG**-3′

where sequences with the same font family and style indicate complementary strands. The underlined AA bases at the center of each sequence constitute the central flexible core. The black (**CGATCG**) self-complementary 6-base overhangs provide the sequences that permit the connection between different DNA-NSs via so-called *sticky-ends*. Bonding between different DNA-NSs is favoured by the inclusion of a nucleotide $\underline{\mathcal{A}}$ immediately before the sticky-end. The non-bonded sequences help releasing angular and rotational constraints, permitting both arm bending and rotation of the end sequences. Depending on the salt-concentration, NSs form at relatively high T and the lifetime of the aggregates becomes essentially infinite at ambient and smaller T. In our case, NSs self-assemble around 65 °C and start to bind to each other below 50 °C.[17]

We prepare the sample dissolving each of the four DNA single strands (provided by IDT already purified in a polyacrylamide gel (PAGE)) in deionized and degassed filtered (0.2 μm filters) H_2O water. Each sample is then centrifuged at 25 °C/4.4 rpm for 5 min to favour the powder dissolution. Up to three different Nanodrop[24] measurements are undertaken to obtain accurate values of the strand concentration. The absorbance measurements (ratios 260/280 = 1.89 and 260/230 = 2.27) confirm the absence of proteins and low concentrations of other contaminants. The resulting solutions are then mingled at proper mixing ratios in order to obtain an equimolar solution of the four different strands. The prepared final concentration was 21 mg/ml, corresponding to 348 μM of NSs. Assuming that each phosphate group releases one counter-ion, then $[Na^+] \approx 63$ mM. The experimental form factor of the DNA-NS required the preparation of a more diluted sample at $c = 3.2$ mg ml^{-1} (53 μM DNA-NS). The diluted sample was prepared in an electrolyte 63 mM NaCl solution to mimic the Na release conditions of the high concentrated sample. This DNA concentration meets the requirements to provide a signal strong enough and consequently a good statistics in the SANS measurements, but at the same time to reduce to a minimum the inter-particle interactions. The resulting samples are heated to 90 °C for 20 min and then cooled down to room temperature in about 7 h. Further details on the preparation can be found in Ref. 18.

B. Small-angle neutron scattering experiments

Comparable volumes, 80 μl, of the two samples were prepared to fill up the quartz Hellma cells (0.5 mm path). In the case of DNA, the contrast provided by H_2O is better than that offered by D_2O. Consequently, measurements were performed using normal water as the solvent and then carefully subtracting the strong incoherent background[25] coming from ^{1}H. SANS measurements of the high concentrated sample were performed at the small-angle diffractometer D22 of the Institut Laue Langevin (ILL, Grenoble, France).[26–28] Using an incident wavelength $\lambda_0 = 6$ Å and suitable sample to detector distances, we explored a wavevector q window from 0.0025 to 0.6 Å^{-1}. Measurements were acquired in a T range from 55 °C to 5 °C. Raw data were treated according to standard procedures, including solvent and empty cell subtraction, using the GRASP software provided by ILL,[29] which yields the value of the scattering intensity onto the absolute intensity scale. In order to test the reversibility of the NS assembling process, the same sample was also probed at the SANS instrument PACE of the Laboratoire Léon Brillouin (LLB, CEA Saclay, France). The instrument configuration allowed us to cover a q-range from 0.02 to 0.6 Å^{-1} and data were analysed with the software PASiNET. Finally, to properly evaluate the form factor $P(q)$, the diluted sample

with $c = 3.2$ mg/ml was measured on the V4 instrument of the neutron source BER II at the Helmholtz-Zentrum Berlin (HZB, Berlin, Germany).[30] Data were acquired at $T = 50\,^{\circ}$C in a q-range from 0.01 to 0.39 Å^{-1}. Standard data reduction was accomplished by means of the BerSANS-PC software.[31]

C. Simulations

We perform molecular dynamics simulations of one isolated NS for different T and salt concentrations to provide the theoretical predictions for the NS form factor. We employ oxDNA2,[32] a coarse-grained model that has been shown to provide a physical representation of the thermodynamic and mechanical properties of single- and double-stranded DNA.[23,33,34] The basic unit of the model is a nucleotide, represented as an oriented rigid body. In oxDNA2, the interaction between nucleotides takes into account the sugar-phosphate backbone connectivity, excluded volume, hydrogen bonding, nearest neighbour stacking, cross-stacking between base-pair steps in a duplex, and coaxial stacking. Hydrogen bonding can occur between complementary bases when they are antialigned, leading to the formation of double-stranded conformations. Electrostatic interactions are included as screened Yukawa repulsions, assuming dissociation of the phosphorous sites. Unfortunately, low ionic-strength simulations of the aggregation process with an accurate DNA model, even at the coarse grained oxDNA2 level, are still unfeasible and a direct comparison between simulations and experiments in non-dilute conditions is not possible. Indeed, under conditions of low ionic strength, repulsive screened electrostatic interactions become long ranged, slowing down the computation beyond what is currently possible. We thus limit ourselves to simulations of isolated DNA NSs, to evaluate their form factor.

In addition, in order to evaluate the form factor of the NS, we need to convert the oxDNA2 representation into a full-atom one. This conversion is crucial to properly reproduce the interatomic distances and therefore their scattering signature in the large-q window. We carry out this procedure by considering that the orientation of each coarse-grained base is identified by three axes. Two of these, $\vec{a}_1$ and $\vec{a}_3$, define the directions along which hydrogen bonding and stacking interactions are maximised. These can be mapped onto an aromatic base by exploiting the planarity of the latter, making it possible to define the atomic analogues of $\vec{a}_1$ and $\vec{a}_3$. This procedure fixes the orientation of the bases. Their positions are then set by superimposing the base site of each coarse-grained nucleotide with the centre of mass of the full-atom aromatic ring and shifting it by 1.13 Å along the a_1 axis. When applied to a perfect double helix, this method reproduces the full-atom phosphate-phosphate distances with a 99.9% accuracy.

We evaluate the normalised numerical form factor $P_{Sim}(\mathbf{q})$ as

$$P_{Sim}(\mathbf{q}) = \frac{1}{\sum_{i,j=1}^{N} b_i b_j} \left\langle \left| \sum_{j=1}^{N} b_j \exp[i\mathbf{q}\cdot\mathbf{t}_j] \right|^2 \right\rangle, \qquad (1)$$

where N is the total number of atoms composing the NS, $\mathbf{t}_j$ is the vector joining the center of mass of the NS to atom j, and b_j the atom scattering length. The average $\langle\cdots\rangle$ is performed over all different orientations and all different configurations generated in the molecular dynamics run (to sample all possible geometrical shapes assumed by the NS).

III. RESULTS AND DISCUSSION

A. Dilute sample: Form factor analysis

Fig. 2 shows the normalized intensity measured at $T = 50\,^{\circ}$C for the sample at $c = 3.2$ mg/ml, compared with $P_{Sim}(q)$. Beyond 0.03 Å^{-1}, the experimental data are very well described by $P_{Sim}(q)$, supporting the quality of the oxDNA force-field in modelling the structure of the NS. The radius of gyration, calculated by the atomic model, corresponds to $R_g = 54$ Å, to be compared with an estimated length of the double helix arms of 68 Å (0.34 Å per base[35]).

Fig. 2 also shows the theoretical form factor of a homogeneous rigid cylinder of radius $r_c = 8$ Å and with length much larger than r_c[36,37]

$$P_{Cyl}(q) \sim \left(\frac{2J_1(qr_c)}{qr_c} \right)^2, \qquad (2)$$

where J_1 is the Bessel function of the first kind. The figure shows that between 0.06 Å^{-1} < q < 0.35 Å^{-1} the experimental data can be quite accurately modeled by $P_{Cyl}(q)$. The 8 Å radius agrees with the value reported in previous small-angle scattering studies of short DNA double helices.[38–40] We ascribe the difference between the 8 Å and the outer diameter of the B-DNA helix (~10 Å) to the assumption of the homogeneous cylinder.[25,40,42–44]

The dissimilarity between $P(q)$ and $P_{Cyl}(q)$ for q < 0.06 Å^{-1} highlights the effects of the inter-arm correlations inside one single NS. While $P_{Sim}(q)$ models rather well the experimental data and captures the extra scattering due to inter-arm correlations, it fails to describe the measurements

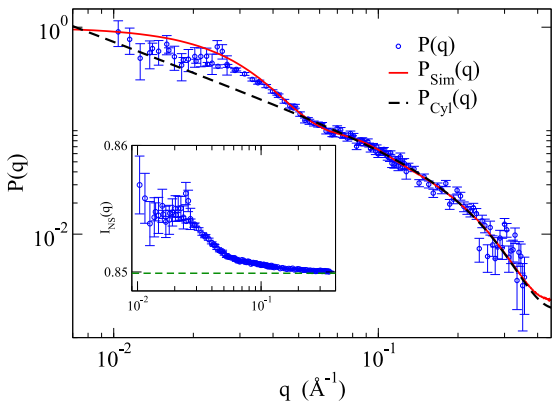

FIG. 2. Normalised experimental $P(q)$ form factor (blue dots), simulated $P_{Sim}(q)$ form factors (solid red line) and theoretical predictions for a cylindrical shape $P_{Cyl}(q)$ (dashed black line), calculated from Eq. (2), assuming an infinite long cylinder with cross section radius $R_c = 8$ Å. The experimental $P(q)$ is obtained from the intensity measured on V4 at 50 °C on the diluted sample ($c = 3.2$ mg/ml). The experimental intensity in absolute units is reported in the inset. The green line represents the level of the background. The numerical form factor $P_{Sim}(q)$ is calculated averaging over an equilibrium ensemble of configurations of an isolated NS at 50 °C and [NaCl] = 0.1 M.

below 0.03 Å^{-1}. In this region the data might be affected by weak but detectable long range electrostatic repulsion among NSs. Indeed, DNA is known to be a highly negatively charged polymer, in which all phosphorous groups are ionised, resulting in a bare net charge of about 200 e per tetramer. The significant DNA charge originates an inter-NS repulsion which is detected even at low density. A precise characterization of the window $q < 0.03$ Å^{-1} would require measurements at lower NS concentrations, where, unfortunately, experiments are not easily performed due to the weak scattering signal.

The quality of the comparison between the experimental and the theoretical structure factor, besides providing a precise characterisation of the geometry of the NS, confirms the high efficiency of the self-assembly process. Electrophoretic gel runs have indeed suggested that more than 95 per cent of the NS properly form.[17]

The agreement between simulations and experimental data offers us the possibility to exploit simulations to quantify the dependence of the NS radius of gyration, R_g, on T and on the salt concentration. The T-dependence is particularly relevant, since it is not possible to perform experiments at low T at dilute concentration due to the onset of the limited-valence gas-liquid like phase separation[17] which takes place in the sample. Luckily, the inset of Fig. 3 reveals that R_g strongly depends on the salt concentration whereas it weakly changes with T. According to the oxDNA2 model, the increase of R_g arises prevalently from the expansion of the central junction, where repulsive forces are non-compensated by complementary base bonding. The predicted salt dependence of $P_{Sim}(q)$ shows the sensitivity of the experimental measurement, which is only consistent with the form factor evaluated at the lowest accessible ionic strength.[32]

B. Gel-forming sample

Previous static and dynamic light scattering studies have focused on the thermodynamic behavior of the NS, providing evidence of a limited-valence phase separation[17] in the low concentration region. At a total $[Na^+] \approx 60$ mM, phase separation extends from very low concentration up to 17 mg/ml. For higher NS concentration the system remains homogeneous at all Ts, forming an open equilibrium-gel structure at low T.[17]

We provide here the first measurement of the structural properties of the system in the equilibrium gel region, covering the range of T (from 55 °C to 5 °C) over which DLS observes an increase of the relaxation time by more than five orders of magnitude, revealing the formation of larger and larger clusters of bonded NSs that eventually span the entire system, forming the gel. The highest investigated T is lower than the T at which the stars unfold ($T_m \approx 65$ °C).

Experimentally, we measured the scattered intensity by the DNA NS in H_2O and the solvent contribution, $I_{sample}(q)$ and $I_{solvent}(q)$, respectively. Under the hypothesis of decoupling between translational and orientational degrees of freedom, the signal coming from the DNA NS can be written as

$$I_{NS}(q) = I_{sample}(q) - \alpha I_{solvent}(q) = \beta P(q) S(q), \qquad (3)$$

where $P(q)$ is the experimental form factor and $S(q)$ is the NS-NS structure factor, resulting from the interparticle interactions of the DNA NSs. The parameter β is defined as $\beta = n v_p^2 (\Delta\rho)^2$, with n the number density of particles, v_p the volume occupied by a NS, and $\Delta\rho$ the particle scattering length density difference between the NS and solvent. Finally, α is a T-dependent fitting factor.

The best value for α has been determined by imposing that in the $0.1 < q < 0.3$ Å^{-1} region the signal from NSs coincides (again apart from the constant β) with the normalized simulated form factor $P_{Sim}(q)$. The best fit values for α are all between 0.99 and 0.96, suggesting a very small T variation of the solvent incoherent scattering. The best fit values of β (defining the value of the form factor in $q = 0$) are found to be $1.4 \leq \beta \leq 1.8$.

Figure 4 shows the resulting $I(q)$ (normalized by β) at all investigated Ts. According to these results, we can differentiate three scattering regions. At low-q values, at the lower limit of the experimental resolution, we observe a significant signal, suggesting the presence of

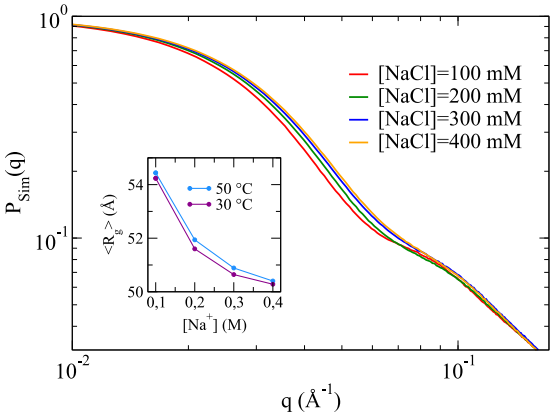

FIG. 3. Ionic strength dependence of the simulated form factor $P_{Sim}(q)$, as obtained by the oxDNA2 model. The inset shows the corresponding radii of gyration R_g for two different T as a function of salt concentration.

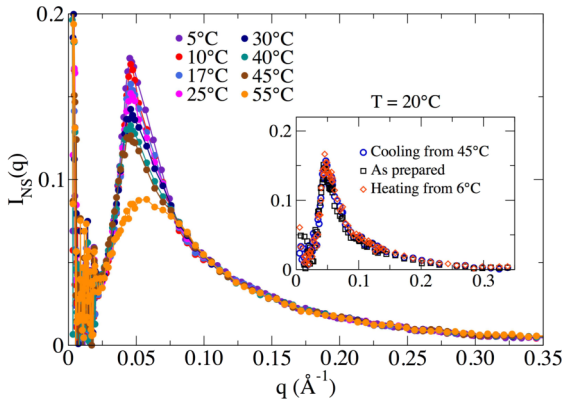

FIG. 4. Temperature evolution of $I_{NS}(q)$ measured on the $c = 21$ mg ml^{-1} sample. Data were acquired at the D22 diffractometer at T varying from 55 °C to 5 °C. The inset (same units) shows three different measurements done at the PACE diffractometer to provide evidence of full reversibility of the assembling process. Data were acquired at 20 °C. The sample was initially measured after a long equilibration (black squares). Subsequently it was re-measured after a cooling scan started from 45 °C (blue circles) and finally re-measured after an heating scan from 6 °C (red diamonds).

correlated scatterers over tens of nanometers. This upturn for $q < 0.02$ Å^{-1}, which is commonly found in polyelectrolyte solutions,[45,46] has been discussed by several authors.[41,47–51] Within this context, the strong low-q signal is usually associated with the recurrent clustering behavior of biological macromolecules, such as DNA.[52–55] In the present case, this tendency is always observed, at all T, even when all NSs are not bounded and hence this very low q peak cannot be associated with inhomogeneities in the gel. We note on passing that DLS has also evidenced the presence of small concentrations of approx 0.1 μm size, which are possibly introduced in the sample during the DNA synthesis. These impurities could be well responsible for this low-q signal.

The most interesting part of the scattered intensity is the region of $q \approx 0.05$ Å^{-1}, where we observe the presence of a peak which increases its amplitude on cooling. The corresponding real-space distance estimated as $d^* = 2\pi/q = 114$ Å is comparable with the center-to-center distance in a pair of bonded NSs (estimated to be about 140 Å), suggesting the possibility to interpret such growth as structural evidence of the progressive formation of the gel, in agreement with the previous DLS measurements of the same DNA NS sample solutions.[18]

For $q > 0.1$ Å^{-1} the intensity does not vary with T anymore and all the curves decay following the form factor.

It is worth noting that the aggregation process of the DNA NSs is fully reversible. This is clearly visible in the inset of Fig. 4, where three measurements at $T = 20$ °C are reported. The first measurement was taken at the sample preparation conditions, whereas the second and third were acquired after cooling the sample down from $T = 45$ °C and heating it up from $T = 6$ °C, respectively.

C. Structure factor analysis

Fig. 5 shows the structure factor $S(q)$ as defined in Eq. (3). The T-dependence of the effective structure factor shows the onset of a peak at a q^{peak} position that shifts to lower q values (see the inset of Fig. 5) as T decreases until it stabilizes at $q^{peak} = 0.0585$ Å^{-1} ($2\pi/q^{peak} = 107.4$ Å) once the gel is formed. $S(q^{peak})$ increases slower and slower on cooling. This behavior, predicted theoretically and supported by numerical calculations, has been observed in the ageing process of a clay gel[56] but never observed experimentally in a controlled and designed thermoreversible system. In the theoretical studies, saturation results from the formation of a fully bonded network of tetravalent particles. In this "ground zero" structure, all possible bonds are essentially formed and structural evolution is completed. Dynamics is still possible via the rare breaking and reforming of the inter-NS bonds on a timescale dictated by the free-energy cost $\Delta G_{breaking}$. This last quantity has been estimated by DLS experiments to be about 1.3 ΔG_{CGATCG}, where ΔG_{CGATCG} is the known[57] binding free energy of the sticky CGATCG sequence. At the lowest investigated T, the bond-breaking timescale is larger than 10 s. Fig. 5 also shows that the system has a very small compressibility (the limit of $S(q)$ for $q \to 0$), as expected for a solution of significantly charged particle at small ionic strength.[58]

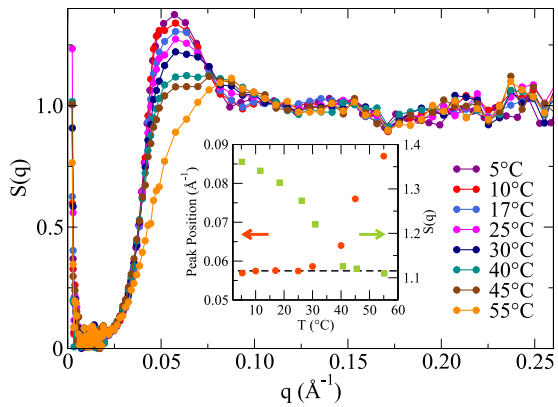

FIG. 5. Static structure factor $S(q)$ at different T (55–5 °C) calculated from the ratio between $I(q)$ and $P_{Sim}(q)$. The shift of the peak position (Å^{-1}) (dark orange dots) and its intensity (light green squares) as a function of T are displayed in the inset.

IV. CONCLUSIONS

We have investigated the aggregation process of self-assembled DNA NSs, generated by mixing equimolar quantities of four properly designed 49-base DNA oligomers. On cooling, these four strands first associate to form a four-arm star with sticky ends, followed by aggregation of these four-functional supramolecules in a thermoreversible gel structure. The dynamics and phase behavior of this interesting biomaterial have been previously investigated via light scattering. When the system forms an highly connected gel, the DLS results do not provide direct structural information. Indeed, the decay times cannot be straightforwardly interpreted in term of characteristic length scales. For the DNA NS gels, the decay of the density-density correlation functions measured in DLS experiments (over a length scale of about 20–100 times larger than the particle size) has been previously interpreted as composed of two contributions, one fast diffusive decay associated with network vibrations at a fixed bonding pattern and a slow component associated with network restructuring. The timescale of this slow process is controlled by the inter-NS bond lifetime.[18]

Here, we provided a structural characterization of the system resulting from the synergy between neutron experiments and computer simulations. Specifically, we reported the first SANS measurement of the form factor and compared it with predictions based on oxDNA2,[32] a nucleotide-level coarse-grained DNA model. The predictions of the model are found to be in very good agreement with the experimental results in the entire wavevector range, allowing us to estimate precisely the shape of the NS. For the investigated low salt concentration, the NS is found to be rather planar, a geometry that minimizes the electrostatic repulsions. Simulations also provide evidence that the T effect on the shape is negligible. By contrast, the ionic strength exerts a strong dependence on the shape of the NS. On increasing salt concentration, the radius of gyration significantly decreases and the four arms fluctuate more freely.

SANS measurements in the equilibrium gel region showed the presence of a peak in the scattered intensity whose amplitude evolves during the aggregation process and appears to level off at the lowest investigated T, suggesting that a structurally complete fully bonded tetrahedral network has been formed. The effective structure factor, evaluated assuming the validity of the relation $S(q) = I(q)/P(q)$, confirms the previous analysis, in agreement with theoretical predictions of simplified colloidal patchy-particle models.[59] Hopefully, a new experiment at significantly large ionic strength (where bulk simulations start to be feasible[60]) will allow us to clarify the dependence of the structural properties and the ionic strength effect on the gel structure. Additional experiments could also assess the validity of the decoupling between translational and orientational correlations and substantiate the interpretation of the effective $S(q)$ as the center-to-center structure factor.

SANS techniques have often been applied to the study of gels composed of polymers[51,61–63] (mostly irreversibly cross-linked[64–68]), proteins,[69–71] or nanocomposite clays,[56,72–74] but not commonly interpreted in terms of form and structure factors even for chemical gels very similar to the present physical one (e.g., the binary system developed by the group of Shibayama based on two four-arm poly(ethylene glycol) polymers[21,75]). Cases for which the form factor was measured include the colloid-polymer suspensions characterized by Shah and Zukoski,[76,77] and the SANS characterization of monoclonal antibody conformations reported by Yearley and Liu[78]. The DNA gel discussed here, built on the base-pair selectivity, represents a realisation of an ideal biocompatible physical gel free of entanglement and defects and with a well defined supramolecular unit. Such monodisperse constituents of the network nodes, together with the possibility to compare the neutron data with the accurate geometry provided by the simulations, are crucial for evaluating an effective gel structure factor.

ACKNOWLEDGMENTS

F.S. and J.F.-C. acknowledge support from ETN-COLLDENSE (No. H2020-MCSA-ITN-2014, Grant No. 642774). F.S., T.B., and F.B. acknowledge support from MIUR-PRIN. L.R. acknowledges support from the Austrian Research Fund (FWF) through the Lise-Meitner Fellowship No. M 1650-N27 and from the European Commission through the Marie Skłodowska-Curie Fellowship No. 702298-DELTAS. F.S. thanks José Teixeira for valuable comments.

We also acknowledge the ILL, LLB, and HZB for beam time allocation and the support on data analysis. This project has received funding from the European Union's Seventh Framework Programme for research, technological development and demonstration under the NMI3-II Grant No. 283883.

[1]M. Yoshida and J. Lahann, ACS Nano **26**, 1101–1107 (2008).
[2]A. Condon, Nat. Rev. Genet. **7**, 565–575 (2006).
[3]M. Patil, D. S. Mehta, S. Guvva *et al.*, J. Indian Soc. Periodontol. **12**, 34–40 (2008).
[4]P. C. Nicolson and J. Vogh, Biomaterials **22**, 3273–3283 (2001).
[5]N. A. Peppas, J. Z. Hilt, A. Khademhosseini, and R. Langer, Adv. Mater. **18**, 1345–1360 (2006).
[6]J. Kopeček, Eur. J. Pharm. Sci. **20**, 1–16 (2003).
[7]D. Costa, A. J. M. Valente, M. Graça Miguel, and J. Queiroz, Colloids Surf., A **442**, 181–190 (2014).
[8]D. Tada, T. Tanabe, A. Tachibana, and K. Yamauchi, J. Biosci. Bioeng. **100**, 551–555 (2005).
[9]A. J. Steckl, Nat. Photonics **1**, 3–5 (2007).
[10]A. J. Steckl, H. Spaeth, H. You, E. Gomez, and J. Grote, Opt. Photonics News **22**, 34–39 (2011).
[11]D. Boneh, C. Dunworth, R. J. Lipton, and J. Sgall, Discrete Appl. Math. **71**, 79–94 (1996).
[12]S. M. Douglas, I. Bachelet, and G. M. Church, Science **335**, 831–834 (2012).
[13]N. C. Seeman, Nature **421**, 427–431 (2003).
[14]Y. W. Kwon, C. H. Lee, D. H. Choi, and J. Il Jin, J. Mater. Chem. **19**, 1353–1380 (2009).
[15]R. M. Zadegan and M. L. Norton, Int. J. Mol. Sci. **13**, 7149–7162 (2012).
[16]P. J. Flory, *Principles of Polymer Chemistry* (Cornell University Press, 1953).
[17]S. Biffi, R. Cerbino, F. Bomboi, E. M. Paraboschi, R. Asselta, F. Sciortino, and T. Bellini, Proc. Natl. Acad. Sci. U. S. A. **110**, 15633–15637 (2013).
[18]S. Biffi, R. Cerbino, G. Nava, F. Bomboi, F. Sciortino, and T. Bellini, Soft Matter **11**, 3132–3138 (2015).
[19]E. Bianchi, J. Largo, P. Tartaglia, E. Zaccarelli, and F. Sciortino, Phys. Rev. Lett. **97**, 168301 (2006).
[20]P. J. Lu, E. Zaccarelli, F. Ciulla, A. B. Schofield, F. Sciortino, and D. A. Weitz, Nature **453**, 499–503 (2008).
[21]T. Sakai, T. Matsunaga, Y. Yamamoto, C. Ito, R. Yoshida, S. Suzuki, N. Sasaki, and M. Shibayama, Macromolecules **41**, 5379–5384 (2008).
[22]F. Bomboi, S. Biffi, R. Cerbino, T. Bellini, F. Bordi, and F. Sciortino, Eur. Phys. J. E **38**, 1–8 (2015).
[23]J. P. Doye, T. E. Ouldridge, A. A. Louis, F. Romano, P. Šulc, C. Matek, B. E. Snodin, L. Rovigatti, J. S. Schreck, R. M. Harrison *et al.*, Phys. Chem. Chem. Phys. **15**, 20395–20414 (2013).
[24]P. Desjardins and D. Conklin, J. Visualized Exp. **45**, e2565 (2010).
[25]R. Borsali, H. Nguyen, and R. Pecora, Macromolecules **31**, 1548–1555 (1998).
[26]C. Dewhurst, Meas. Sci. Technol. **19**, 034007 (2008).
[27]See https://www.ill.eu/instruments-support/instruments-groups/instruments/d22/description/instrument-layout/ for detailed information of the diffractometer D22 at the ILL (Last checked: July 2016).
[28]A. Paciaroni, F. Bomboi, L. Comez, J. Fernandez Castanon, L. Porcar, and F. Sciortino, Institut Laue Langevin (ILL), doi:10.5291/ILL-DATA.9-13-559, 2015.
[29]C. Dewhurst, GRASP User Manual V.2, Software V. 3.40, ILL, 2003.
[30]U. Keiderling and A. Wiedenmann, Physica B **213**, 895–897 (1995).
[31]U. Keiderling, Appl. Phys. A **74**(Suppl. 1), S1455–S1457 (2002).
[32]B. E. Snodin, F. Randisi, M. Mosayebi, P. Šulc, J. S. Schreck, F. Romano, T. E. Ouldridge, R. Tsukanov, E. Nir, A. A. Louis *et al.*, J. Chem. Phys. **142**, 234901 (2015).
[33]T. E. Ouldridge, A. A. Louis, and J. P. Doye, J. Chem. Phys. **134**, 085101 (2011).
[34]P. Šulc, F. Romano, T. E. Ouldridge, L. Rovigatti, J. P. Doye, and A. A. Louis, J. Chem. Phys. **137**, 135101 (2012).
[35]R. A. Jones, *Soft Condensed Matter* (Oxford University Press, 2002), Vol. 6.
[36]K. Kassapidou, W. Jesse, M. Kuil, A. Lapp, S. Egelhaaf, and J. Van der Maarel, Macromolecules **30**, 2671–2684 (1997).
[37]A. Guinier and G. Fournet, *Small-Angle Scattering of X-Rays* (John Wiley and Sons, 1955).
[38]J. R. C. van der Maarel and K. Kassapidou, Macromolecules **31**, 5734–5739 (1998).
[39]J. R. C. van der Maarel, Biophys. J. **76**, 2673–2678 (1999).
[40]H. Lederer, R. P. May, J. K. Kjems, and H. Heumann, Eur. J. Biochem. **161**, 191–196 (1986).
[41]J. D. Watson and F. H. C. Crick, Nature **171**, 737–738 (1953).
[42]V. Luzzati, F. Masson, A. Mathis, and P. Saludjian, Biopolymers **5**, 491–508 (1967).
[43]J. Garcia de la Torre and A. Horta, J. Phys. Chem. **80**, 2028–2035 (1976).
[44]M. H. J. Koch, Z. Sayers, P. Sicre, and D. Svergun, Macromolecules **28**, 4904–4907 (1995).
[45]M. Milas, M. Rinaudo, R. Duplessix, R. Borsali, and P. Lindner, Macromolecules **28**, 3119–3124 (1995).
[46]N. Arfin, V. K. Aswal, J. Kohlbrecher, and H. B. Bohidar, Polymer **65**, 175–182 (2015).

[47]M. Sedlak, J. Chem. Phys. **105**, 10123–10133 (1996).
[48]M. Shibayama, Macromol. Chem. Phys. **199**, 1–30 (1998).
[49]H. Matsuoka, D. Schwahn, and N. Ise, Macromolecules **24**, 4227–4228 (1991).
[50]Y. Zhang, J. F. Douglas, B. D. Ermi, and E. J. Amis, J. Chem. Phys. **114**, 3299–3313 (2001).
[51]M. Sedlak, J. Chem. Phys. **116**, 5256–5262 (2002).
[52]K. Dusek and W. Prins, Adv. Polym. Sci. **6**, 1–102 (1969).
[53]E. Geissler, A. Hecht, and R. Duplessix, J. Polym. Sci., Polym. Phys. Ed. **20**(2), 225–233 (1982).
[54]E. Geissler, F. Horkay, and A. Hecht, Phys. Rev. Lett. **71**, 645 (1993).
[55]J. M. Guenet, M. Kein, and A. Menelle, Macromolecules **22**, 494 (1989).
[56]B. Ruzicka, E. Zaccarelli, L. Zulian, R. Angelini, M. Sztucki, A. Moussaïd, T. Narayanan, and F. Sciortino, Nat. Mater. **10**, 56–60 (2011).
[57]J. SantaLucia, Proc. Natl. Acad. Sci. U. S. A. **95**, 1460–1465 (1998).
[58]J. R. Van der Maarel, *Introduction to Biopolymer Physics* (World Scientific, 2008).
[59]F. Sciortino and E. Zaccarelli, Curr. Opin. Solid State Mater. Sci. **15**, 246–253 (2011).
[60]L. Rovigatti, F. Bomboi, and F. Sciortino, J. Chem. Phys. **140**, 154903 (2014).
[61]S. Chaterji, I. K. Kwon, and K. Park, Prog. Polym. Sci. **32**, 1083–1122 (2007).
[62]L. Z. Rogovina, V. G. Vasil'ev, and E. E. Braudo, Polym. Sci., Ser. C **50**, 85–92 (2008).
[63]T. Rossow and S. Seiffert, Polym. Chem. **5**, 3018–3029 (2014).
[64]T. Matsunaga, T. Sakai, Y. Akagi, U.-i. Chung, and M. Shibayama, Macromolecules **42**, 6245–6252 (2009).
[65]L. H. Lee, *Xerox Coorp*, 1st ed. (Plenum Press, 1989), pp. 483–495.
[66]H. Benoit, D. Decker, C. Duplessix, C. Picot, and P. Rempp, J. Polym. Sci., Polym. Phys. Ed. **14**, 2119–2128 (1976).
[67]R. Ullman, Macromolecules **15**, 1395–1402 (1982).
[68]H. M. Tsay and R. Ullman, Macromolecules **21**, 2963 (1988).
[69]A. M. Jonker, D. W. P. M. Löwik, and J. C. M. van Hest, Chem. Mater. **24**, 759–773 (2012).
[70]J. D. Ehrick, S. K. Deo, T. W. Browning, L. G. Bachas, M. J. Madou, and S. Daunert, Nat. Mater. **4**, 298–302 (2005).
[71]S. Tang, M. Wang, and B. D. Olsen, J. Am. Chem. Soc. **137**, 3946–3957 (2015).
[72]P. Li, Siddaramaiah, N. H. Kim, S. B. Heo, and J. H. Lee, Composites, Part B **39**, 756–763 (2008).
[73]C. W. Chang, A. Van Spreeuwel, C. Zhang, and S. Varghese, Soft Matter **6**, 5157–5164 (2010).
[74]L. Z. Zhao, C. H. Zhou, J. Wang, D. S. Tong, W. H. Yu, and H. Wang, Soft Matter **11**, 9229–9246 (2015).
[75]M. Shibayama, Polym. J. **43**, 18–34 (2011).
[76]S. Shah, Y. Chen, S. Ramakrishnan, K. Schweizer, and C. Zukoski, J. Phys.: Condens. Mater. **15**, 4751 (2003).
[77]S. Shah, S. Ramakrishnan, Y. Chen, K. Schweizer, and C. Zukoski, Langmuir **19**, 5128–5136 (2003).
[78]E. J. Yearley, I. E. Zarraga, S. J. Shire, T. M. Scherer, Y. Gokarn, N. J. Wagner, and Y. Liu, Biophys. J. **105**, 720–731 (2013).